P- and S-Wave Velocity Measurements and Pressure Sensitivity Analysis of AVA Response

Tiewei He*
University of Alberta, Edmonton, Alberta, Canada
tieweihe@phys.ualberta.ca

and

Douglas Schmitt
University of Alberta, Edmonton, Alberta, Canada

Abstract

Reservoir conditions, such as the pore pressure and the fluid saturation levels, will change during the production of fluids and enhanced oil recovery. These changes will also influence the seismic wave properties of the rock. In order to better understand its seismic response, compressional and shear wave velocities were measured on a series of low porosity conglomerates under different confining and pore pressures and under both dry and water saturated conditions using standard pulse transmission methods. As expected, the dry P-wave velocities always increase after the dry sample is saturated with water. Conventional assumptions from Gassmann's relations suggest that the S-wave velocity would drop after water saturation; however, in this study an increase of S-wave velocity was observed. The contradiction of the observed data with the theory has been attributed to a number of mechanisms, such as viscous coupling, the reduction in free surface energy, and frequency dispersion due to local flow of the fluid in the microcracks. To better understand the time-lapse seismic data, we also performed the pressure sensitivity analysis of the P-P and P-SV reflectivity on a simple two layer interface using complete Zoeppritz's equations based on the laboratory velocity measurement. The result suggests that both of the P-P and P-SV reflections are very sensitive to the effective pressure.

Introduction

Velocities of rocks generally decrease with increasing porosity for certain kind of rock. However, this velocity-porosity relationship becomes complicated when micro-cracks exist in the rocks, because the elastic properties of a rock are more affected by the micro-cracks than by more open porosity (e.g., Kuster and Toksöz, 1974). Most rocks in the upper crust contain cavities with shapes ranging from spherical to planar microcracks and grain contacts. The presence of flat, low aspect ratio intra- or inter-grains can have a pronounced effect on the elastic properties, even though they have little contribution to the total porosity (Brace, et al. 1972). Moreover, the surface area of the low aspect ratio pores and cracks becomes more important than the porosity itself when the sample is saturated with fluid (Tatham, 1982), therefore, the microcracks will also complicate fluid substitution theory. The evolution of the more compliant microcracks depends on

the changes of the pore pressure and confining pressure. The establishment of the pressure and elastic properties is of great interest for the geophysicist to understand the seismic properties of producing reservoir. In order to better understand effect of pore and confining pressure on the elastic properties, compressional and shear wave velocities were measured on a series of low porosity conglomerates under different confining and pore pressures and under both dry and water saturated conditions using standard pulse transmission methods.

Frequency dispersion has limited the use of the ultrasonically determined P- and S-wave velocity of fluid saturated rock sample to the seismic exploration. However, it has been a consensus that the bulk and shear modulus determined from laboratory measured P- and S-wave velocities on dry samples can be directly used in fluid substitution at seismic frequency. Based on the P- and S-wave velocity measurement on dry samples, the low frequency seismic velocities can be calculated from the effective bulk moduli (K_{eff}) according to Gassman's formula (Gassman 1951) assuming that the shear modulus is not changed by liquid saturation:

$$K_{eff} = K_d + \frac{(1 - K_d / K_s)^2}{\frac{1 - K_d / K_s - \phi}{K_s} + \frac{\phi}{K_f}}$$

where ϕ is the porosity, K_d, K_f and K_s are the bulk moduli of dry frame, the fluid, and the minerals, respectivly. To better understand the time-lapse seismic data, we also performed the pressure sensitivity analysis of the P-P and P-SV reflectivity on a simple two layer interface using complete Zoeppritz's equations based on the laboratory velocity measurements.

Experimental procedure

The conventional pulse transmission method was used to determine P-wave and S-wave velocity. This method uses transducers made with piezoelectric ceramics to send an ultrasonic wave through the sample, where corresponding transducers on the other end of the sample then pick up the signal. In this experiment, both the compressional and shear wave transducers had a resonant frequency of 1 MHz. The newly updated experimental configuration (Figure 1) now consists of two pressure systems, a confining pressure system and a pore pressure system, where pore fluids can be introduced and their pore fluid pressure can be varied as needed. The new pore pressure system is used to simulate pressure changes in gas & oil reservoirs. The parallel surfaces of the core samples used here were machined parallel to much better than 0.02 mm. Sample preparation consists of placing aluminum buffer caps with P and S wave transducers on each end of the cylindrical sample. This arrangement is then hermitically sealed. The prepared sample is then put in a pressure vessel filled with hydraulic oil for velocity measurement. Before the velocity measurement of the dry sample, a vacuum is used to pump out the air in the samples. After completion of dry velocity measurement, the sample is then saturated with water using the pore pressure setup. Our updated high pressure instrument not only adds pore pressure variations as a variant in monitoring velocity changes but also improves the precision of the velocity measurement by eliminating the effect of time delay and system time shift. The first extremum (peak or trough) was here defined to be the sample transit time. The velocity determined is simply the quotient of the sample length and transit time, estimated uncertainties are typically less than 1%.
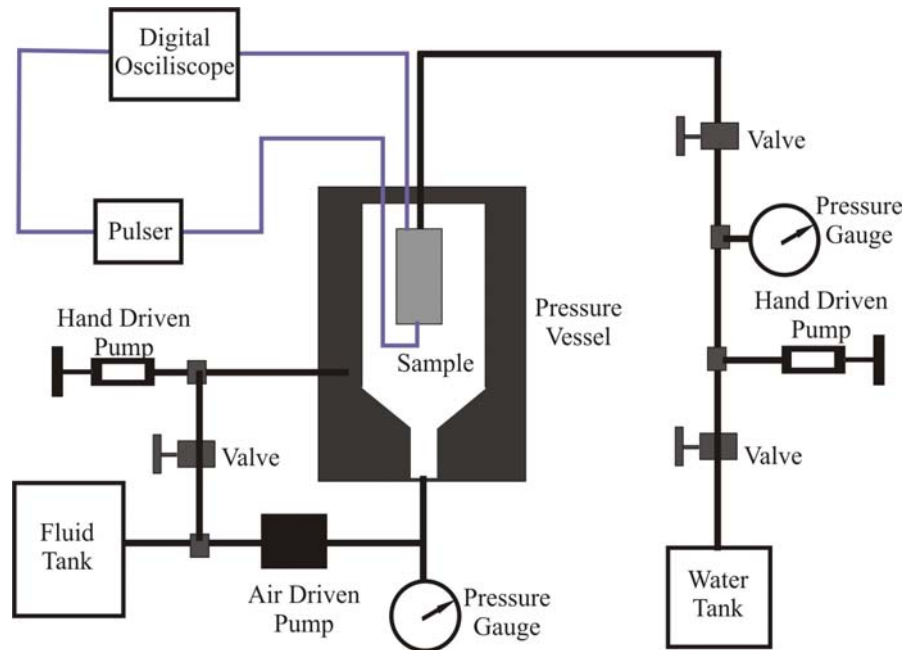
Figure 1. The experimental configuration mainly consists of the confining pressure system, the pore pressure system and the signal acquisition system

Experimental results

The full set of normalized P- wave waveforms of dry sample SB007 is given in Figure 2. The sample is subjected to pressurization from 5MPa to 60MPa and then depressurization from 60MPa to 5MPa. From figure 2, we can see that the waveforms display a remarkable reduction of travel time with the increase of confining pressure, which means the S-wave velocity increases with effective pressure. This is not unexpected as the velocities of such material are known to be highly dependent on the effective stress. The red arrow pointing to the first amplitude extreme of the signal is where we chose the transit time though the sample.

Figure 3 shows the experimentally measured and Gassmann's equation calculated P- and S-wave velocities on the dry and water saturated sample. As expected, the dry P-wave velocities always increase after the dry sample is saturated with water, although the P-wave velocity at low pressures are much higher than that predicted by Gassmann's equation. In contrast to the theoretical prediction, which predicts that the S-wave velocity for the water saturated sample is always lower than that for the dry sample, this figure also shows an unexpected S-wave velocity increase after water saturation at lower effective pressure. At higher effective pressures, the S-wave velocity-pressure curve of the dry rock cross over with that of the water saturated rock at 50 MPa and approaches to the theoretical values. The contradiction of the observed data with the theory has been attributed to a number of mechanisms, such as viscous coupling, the reduction in free surface energy, and frequency dispersion due to local flow of the fluid in the microcracks. This further demonstrates that the microcacks not only plays an important roll in controlling the pressure dependency of velocity but also has a large effect on the fluid substitution.

Contrary to the confining pressure, the pore pressure generally decreases the wave velocities and rock stiffness (Figure 4). At constant differential pressure, both of the P- and S-wave velocities hardly increase with the increasing confining pressure. The combining effect of internal pore pressure and confining pressure on the elastic wave velocities leads to an effective pressure that can be expressed as $P_e=P_c-nP_p$, where n is the effective stress coefficient close to 1. When the internal pore pressure (P_P) exactly cancel the effect of the confining pressure (P_c), this equation can be reduced to $P_e=P_c-P_p$ with the effective stress coefficient being 1.

Figure 5 shows P-P and P-Sv reflection coefficient as a function of angle of incidence and effective pressure. The velocities used in the lower layer are the Gassmann's equation predicted velocities of the water-saturated sample (SB007); the velocity and density of the upper layer is assumed to be a shale layer with constant velocity and density. The P-P reflection coefficient increases remarkably with increasing effective pressure at the low angle of incidence; however, it hardly changes with effective pressure at the higher angle of incidence. Therefore, the PP reflection coefficient is more sensitive to effective pressure at the low-pressure areas. In contrast, the angle dependency is much stronger at high-pressure area. Contrary to the PP reflection coefficient, the P-SV reflection coefficient shows little changes with the variation of effective pressure at low angle of incidence; but it shows remarkable changes at high angle of incidence. Just the same as the P-P reflection coefficient, the angle dependency of P-SV reflection coefficient is more obvious at high effective pressure.
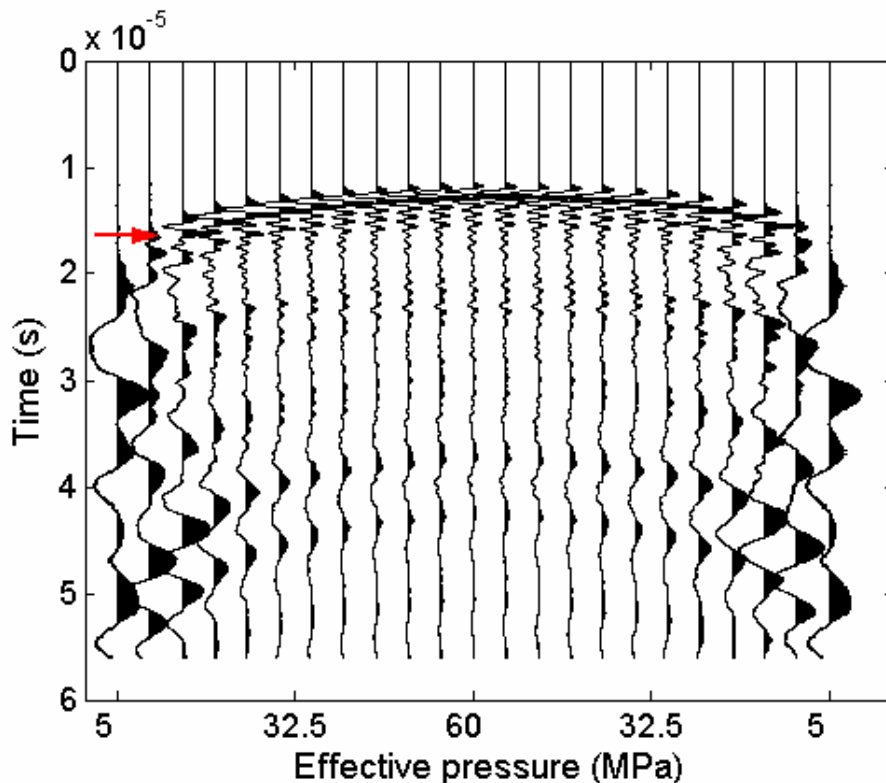

Figure 2. The waveform of P-wave traces of the dry sample SB007. The red arrow pointing to the first amplitude extreme of the signal is where we pick up the transit time though the sample.
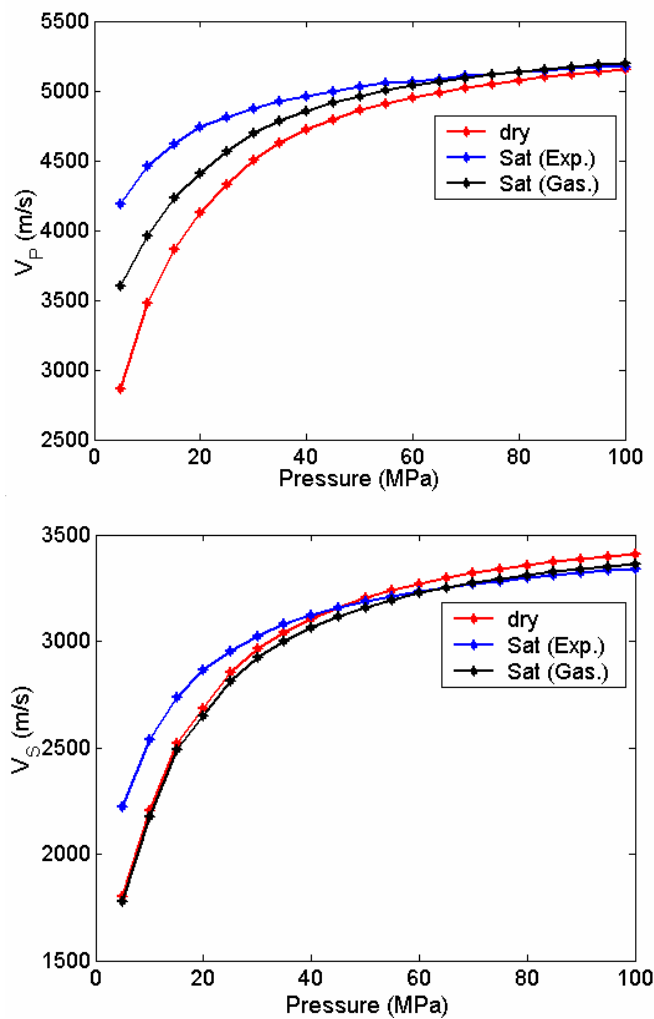
Figure 3. The experimentally measured and Gassman's equation calculated P- (left) and S-wave (right) velocities on the dry and water saturated sample.
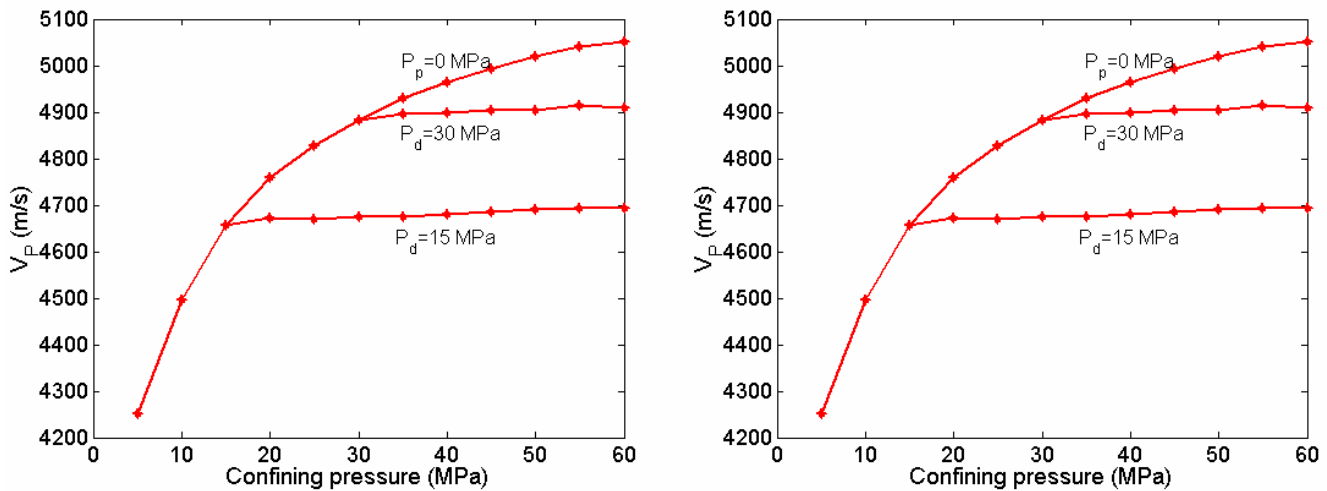
Figure 4. P- and S-wave velocity as a function of confining pressure and differential pressure for water saturated sample SB007.
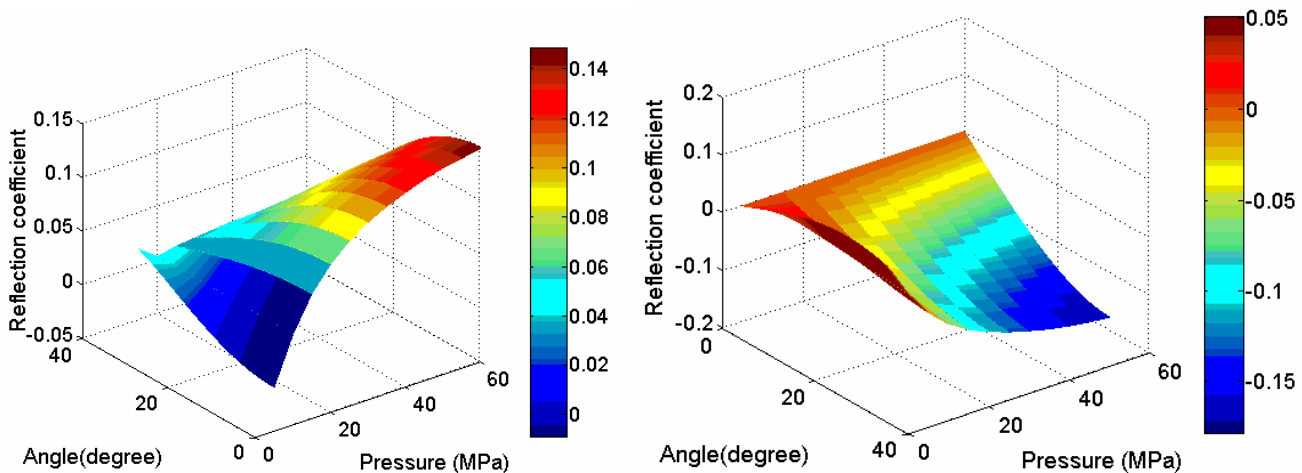

Figure 5. P-P (left) and P-SV (right) reflection coefficients as a function of angle of incidence and effective confining pressure. The V_P, V_S and density of the upper layer are 4000m/s, 2300m/s and 2300kg/m^3 respectively; the velocities in the lower layer are the Gassmann's equation predicted velocities of the water-saturated sample (SB007)

Conclusion

Both of the P- and S-wave velocities increase sharply at low effective pressure and then tend to stabilize at higher pressures. According to Gassmann's equation, the P-wave velocity will increase and the S-wave velocity slightly decreases due to the density changes after fluid saturation. However, we see a noticeable increase of the S-wave after water saturation at low effective pressure. Both of the experimentally measure P- and S-wave at ultrasonic frequencies are much higher than the Gassmann's equation calculated velocities at lower effective pressures. The deviation of the experimental velocities from the theoretical values can be attributed to the frequency dispersion and the microcracks leading to local fluid flow. From the experiments, we find the pore pressure has an opposite effect to the confing pressure on the P- and S-wave velocities.

The increases of pore pressure almost but cannot completely cancel the equal amount of confining pressure increases. The pressure sensitivity analysis of the reflection coefficient of suggests that both of the P-P and P-Sv reflection are very sensitive to the effective pressure.

References

Brace, W.F., Silver, E., Hadley, K., and Goetze, C., 1972, Cracks and pores: A closer look: Science, V. 178, 162-764.

Gassmann, F., 1951, Elasticity of porous media: Uber die Elastizitat poroser Medien: Vierteljahrsschrift der Naturforschenden Gesselschaft in Zurich 96, 1-23.

Kuster, G.T., and Toksöz, M. N., 1974, Velocity and attenuation of seismic waves in two-phase media—Pat I: Theoretical formulations: Geophysics, 39, 447-472.

Tatham R. H., 1982, Vp/Vs and lithology: Geophysics, 47,336-344.